Chapter 6

An Integrated Approach to Assess the Impacts of Climatic and Land Use/Cover Changes on the Hydrological Cycle at the Mesoscale Level

6.1 Introduction

As was stated before, the present state of land use in a given spatial unit or region is the outcome of two complex and interacting dynamic systems, namely: the anthropogenic activities and 'natural' subsystems as depicted in Figures 1.1 and 1.2. Hence, land use changes cannot be understood completely without an 'insight' into the innumerable relationships among all possible driving forces that may cause a transformation from a land use/cover into another one.

It is, however, unrealistic to pursue a model that attempts to find all possible links (most of them non-linear) between all processes (e.g. weather conditions, soil type distribution, hydrological regime) and all actors involved (e.g. individuals, firms, government acting according to a legal framework) because of the tremendous size of such a model, which, in turn, would make the analysis so complicated and inefficient that the whole modelling effort would become worthless. In physics, for instance, this sort of determinism has been abandoned a long time ago, especially for the analysis of macroscopic multi-particle systems. A good example is the Metropolis algorithm (Metropolis et al. 1953), which simulates the evolution of a system in a heat bath towards thermal equilibrium. Moreover, in the present case, this amount of information will never be collected because of both economic reasons and data protection laws.

It is possible, nevertheless, to simplify the system's complexity to some extent. For instance, Allen (1978-1997) and Peréz-Trejo (1996) introduced a spatial dynamic modelling framework, which describes the average behaviour of an individual or a firm by a system of interacting differential equations that govern the structural changes of the system with regard to population and employment growth (in various sectors), as well as their spatial distribution. In this case, the system's self-organization is assured by the existence of bifurcation points (a critical point at which the system will branch into completely different paths or possible future states), which in a way preserve the adaptability and creativity of the system according to Allen (1997).

This approach has, however, some shortcomings. Firstly, the fact that most dynamical systems have a strange attractor in some region of the parameter values describing the system (Casti, 1990). Such an

attractor is characterized by instability in all motions, deterministic randomness, and sensitivity to initial conditions. These characteristics imply that a small nudge in one of its variables will take the system to a completely different course. Secondly, the mathematical structure of the system is deterministic; hence, the inherent uncertainty of various subsystems has not been taken into account.

The intrinsic randomness of the system is evident, for instance, when one tries to model the weather conditions in a given area or the housing location choice of an individual. Because of this important characteristic of the system, only one fact is certain: a perfect prediction of a future state based on the present state is impossible.

Based on the previous considerations the following questions may be stated. How can a dynamic system be formalized in order to avoid the aforementioned difficulties and take into account its intrinsic randomness? Moreover, which kind of answers should be expected from this type of model? The consensus found in the reviewed literature points out that this sort of system can be modelled using a mathematical construct named a stochastic process. The technique used for solving such systems is called a stochastic or a Monte Carlo simulation (Hammersley and Handscomb 1964, Ripley 1987, Haldorsen and Damsieth 1990).

This technique employs batches of artificial data (i.e. realizations) generated for every random variable of the model resampled from their corresponding probability distributions. The numerous solutions of the system would allow determining the PDFs of the output variables, from which decisions can be taken in a probabilistic way.

These ideas and their application to assess impacts of land use/cover change on the hydrological cycle in a given basin will be illustrated with the following stochastic simulation model.

6.2 Model Structure

The model presented here consists of four modules (see Figure 6.1):

1. The land use/cover change model,
2. The scenario definition,
3. The stochastic simulation, and
4. The statistical inference.

It should be noted that the model structure is general and, hence, it can be applied anywhere. However, the calibration of the land use/cover change model, as well as, modules two and four depend on local conditions that have to be analysed for each particular case. Therefore, they will be discussed extensively in Section 6.3 which deals with the model implementation in the Special Study Area.

6.2.1 A Simple Land Use/Cover-Change Model

The land use/cover change (LUCC) model described below has been chosen because it has a simple structure and can be implemented easily. Furthermore, it assumes that there exists a one to one relationship between each land use and land cover class employed. Despite its simplicity, this model still captures key components that characterize the complexity of the real phenomenon as will be

shown in the next section. This model is based on works carried out by Bell (1974), Turner (1987), Flamm and Turner (1994), and, Muller and Middleton (1994). This model can be further improved by considering the spatial variability of the land cover transitions (e.g. by using semivariograms) as has been proposed recently by Brown (2002). In this respect, more research is still needed.

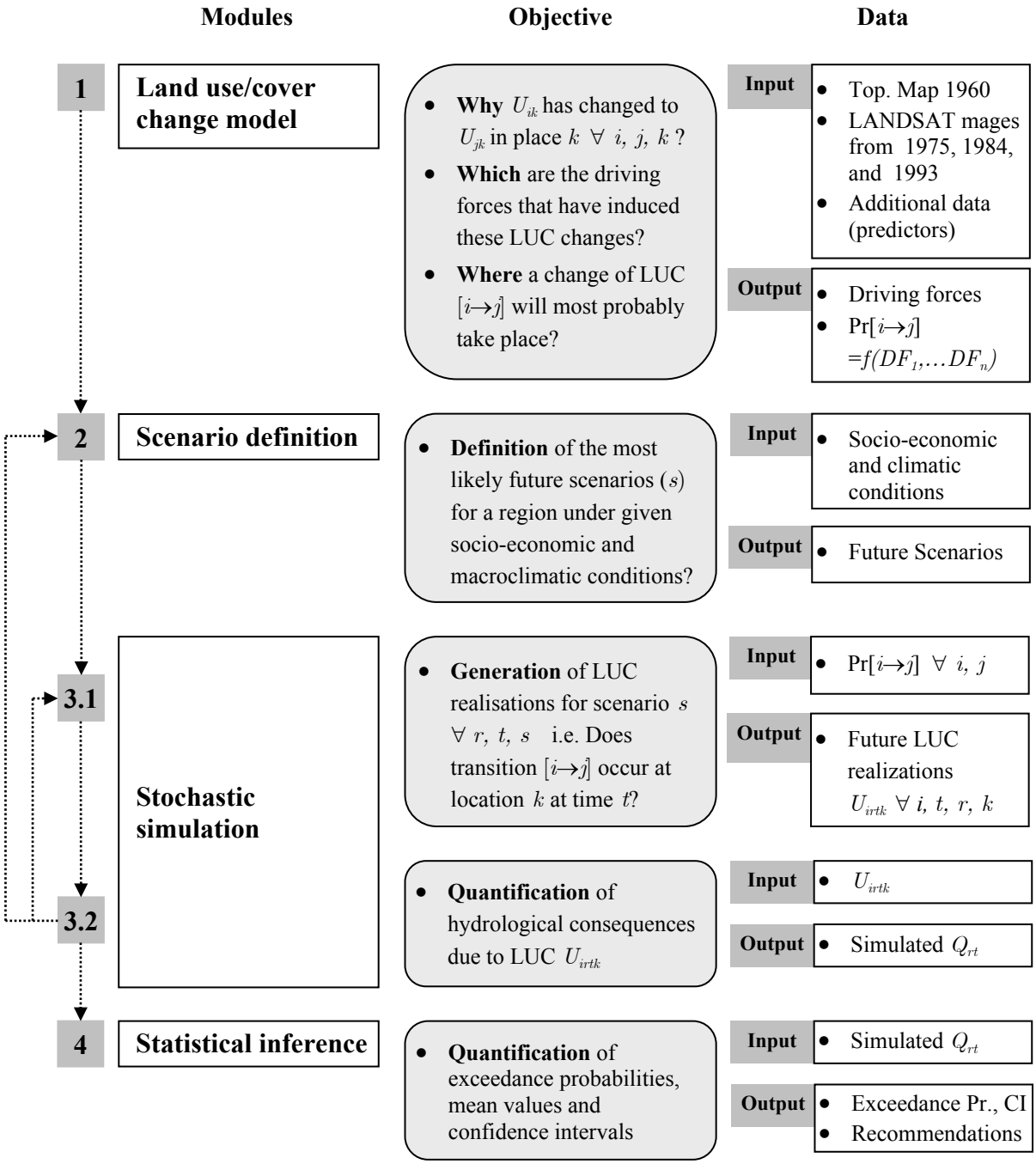

Figure 6.1 Model structure showing the main objectives, required inputs, and outputs for each module.

Let the pair $(\mathbf{Z}, \boldsymbol{F})$ be a stochastic process resembling the land use/cover transformations to be endured by the system during a time span T. Let $\mathbf{Z} = \{(i,j) : 1 \le i,j \le N\})$ denote the $N \times N$ integer lattice covering a given spatial unit Ω ; then $\mathbf{U}^t = \{U_{ij}^t\}, (i,j) \in \mathbf{Z}$ denotes the land use/cover of spatial unit Ω at time t, where $t = 1,\ldots,T$. Let $\mathbf{S} = \{s_q : q = 0,1,\ldots,u\} = \{0,1,\ldots,u\}$ be a finite state space

denoting $u+1$ mutually exclusive land use/cover classes so that $U_{ij}^{t} \in \mathbf{S}\ \forall\, i,j,t$. Finally, let $\boldsymbol{\mathcal{F}} = \{\boldsymbol{\mathcal{F}}_{ij}\}, (i,j) \in \mathbf{Z}$ be a neighbourhood system where $\boldsymbol{\mathcal{F}}_{ij} \subseteq \mathbf{Z}$ denotes the neighbours of (i,j).

Then, the system can be defined as a Markov random field[1] over $(\mathbf{Z}, \boldsymbol{\mathcal{F}})$ if for every (i,j) and every s_q (see Geman and Geman, 1984)

$$\begin{aligned}\Pr(U_{ij}^{t} = s_{q'} \,\big|\, U_{kl}^{t-1} = s_{q_{kl}}^{t-1},\ \forall (k,l) \in \mathbf{Z},\ t = 1,\ldots,t-1) \\ = \Pr\left(U_{ij}^{t} = s_{q'} \,\middle|\, U_{kl}^{t-1} = s_{q}^{t-1}, \left((k,l) \in \boldsymbol{\mathcal{F}}_{ij} \vee (k,l) = (i,j)\right)\right), \\ = (\pi_{qq'})_{ij}^{t}.\end{aligned} \tag{6.1}$$

where $(\pi_{qq'})_{ij}^{t}$ is the probability that the outcome of the t-th transition in cell (i,j) will be $s_{q'}$, given that the outcome of the $t-1$-th transition was s_q, and $s_q, s_{q'} \in \mathbf{S}$. In other words, the system has no memory; the selection of the new state (t) for a given cell (i,j) depends only on the current state $(t-1)$ of this cell and its neighbours and not on prior states. Since historical records support this condition, the system is fully determined by the transition-probability matrix $\boldsymbol{\Pi}(\pi_{qq'})_{ij}^{t}$ given by

$$(\pi_{qq'})_{ij}^{t} = \begin{cases} 0 & q = 0 \vee q' = 0 \\ p_{ij}^{t}(q,q') & \forall q \neq q'\ \ q,q' \geq 1 \\ 1 - \sum_{\substack{l=0 \\ l \neq q}}^{u} p_{ij}^{t}(q,l) & q = q' \end{cases}. \tag{6.2}$$

Turner (1987), Brown (2000, 2002), among others, have pointed out that the transition probability $p_{ij}^{t}(q,q')$ depends on local and time specific conditions. Several empirical studies also have shown that the transition probability is related with socio-economic factors, land use policies, and morphological characteristics of the terrain (Bell, 1974; Flamm and Turner, 1994; Berry, 1995; Brown et al. 2000, 2002).

In the present case, this probability will be determined by (based on Berry et al. 1995)

$$p_{ij}^{t}(q,q') = w_0(q,q')\, w_P(q,q')\, w_{ij}^{t}(q,q') \frac{\exp\left(\beta_0(q,q') + \sum_{k=1}^{K} \beta_k(q,q') x_k(i,j)\right)}{1 + \sum_{\substack{l=1 \\ l \neq q}}^{u} \exp\left(\beta_0(q,l) + \sum_{k=1}^{K} \beta_k(q,l) x_k(i,j)\right)} \tag{6.3}$$

$$\forall q \neq q'\ \ q,q' \geq 1\ ,$$

where

$w_0(q,q')$ = Calibration and scaling parameters to be determined with past information.

$w_P(q,q')$ = Control parameters denoting both the political willingness and the society's level of awareness with regard to environmental impacts and sustainability. The

---

[1] A Markov random field (MRF) is a stochastic process regarded as a generalization of the usual Markov chain (Cross and Jain, 1983). A Markov chain is a sequence of trials, where the outcome of each trial depends only on the outcome of the previous one (Feller, 1950 quoted by van Laarhoven and Aarts, 1992).

set of parameters will be scenario specific and will be of key importance during the simulation. In general, they are values greater or equal to zero. Zero means that a transition is not possible and the greater the value, the greater the willingness to promote such transformation.

$w_{ij}^{t}(q,q')$ = Location and time specific factor indicating the likelihood that a given cell will be transformed to another land use/cover type based on the neighbourhood conditions.

K = Number of exogenous variables regarded as driving forces behind a land use/cover change.

l,k,i,j = Indexes.

$x_k(i,j)$ = Time independent driving force k, with $(i,j) \in \mathbf{Z}$.

$\beta_0(q,q')$ = Intercept for a LUCC from $q \rightarrow q'$.

$\beta_k(q,q')$ = Coefficient estimate for driving force k related with a LUCC from $q \rightarrow q'$.

This probability assumes that the driving forces will be constant or quasi-constant during the simulation time, and it takes into account the fact that landscape changes do not occur randomly in space but in patches or clusters (Brown, 2002). In other words, if a given cell is surrounded by cells belonging to a distinct land use/cover class it is more likely that a land use/cover change occurs here rather than in another one that is surrounded by the same land use/cover class.

The variable $w_{ij}^{t}(q,q')$ has been estimated as

$$w_{ij}^{t}(q,q') = \frac{\left|\left\{(i,j) : U_{ij}^{t-1} = s_{q'} \wedge (i,j) \in \boldsymbol{\mathcal{F}}_{ij}\right\}\right|}{n_c + 1}, \tag{6.4}$$

where $|\{\cdot\}|$ represent the cardinality of the set composed of all neighbours of the cell (i,j) having a land use/cover type q' at the $t-1$-th transition. n_c denotes the number of neighbours of a given cell and c an integer denoting the neighbourhood configuration. In the present case $c = 2$, which means that a given cell has eight neighbours (i.e. $n_c = 8$). The neighbourhood is determined as in Geman and Geman (1984)

$$\boldsymbol{\mathcal{F}}_{ij} = \left\{(k,l) \in \mathbf{Z} : 0 < (k-i)^2 + (l-j)^2 \leq c\right\}. \tag{6.5}$$

6.2.2 Stochastic Simulation

The purpose of the stochastic simulation is to determine how severely a change in land use/cover would affect the hydrological system of a given basin Ω provided specific scenario conditions. The impacts on the hydrological system will be quantified by those empiric models calibrated in Chapters 4 and 5. The variables used by these models will be obtained as follows. The land use/cover variables are obtained as realizations of the LUCC model proposed before; the morphological variables are invariants for the period of the simulation; and the climatic variables will be drawn from their multivariate joint distribution. The resampling procedure, however, has to be done sequentially since the climatic variables are mutually dependent. The procedure is as follows. Firstly, a variable assumed

to be independent (i.e. either x_{24}, x_{25}, or x_{27}, for winter, summer and annual respectively) has to be drawn from their respective EDF. For a subsequent variable, however, the distribution from which it has to be drawn will be modified by the value of the primary variable. This modified distribution is the conditional distribution as defined by the Bayes theorem. The conditional distribution for a secondary variable x_k can be formally written as

$$F_{X_k|X_i,\forall i\neq k}(x_k\,|x_i,\forall i\neq k)=\Pr(X_k\leq x_k\,|X_i=x_i,\forall i\neq k)\,. \tag{6.6}$$

The proposed simulation is carried out by the subsequent algorithm.

Algorithm 6

1. For $r=1,\ldots,R$, where R denotes the total number of realizations.
2. For $t=1,\ldots,T$, where T denotes the total number of years in each realization r.
3. For all $(i,j)\in\mathbf{Z}$.
   a. Estimate $p_{ij}^{t}(q,q')$ as in (6.3).
   b. Generate a random number $\varpi\sim\mathrm{unif}[0,1)$.
   c. If $\sum_{l=1}^{q'-1}p_{ij}^{t}(q,l)<\varpi\leq\sum_{l=1}^{q'}p_{ij}^{t}(q,l)$ accept transition from $q\rightarrow q'$.
4. Estimate land use/cover shares $\mathbf{U}_{\Omega r}^{t^*}$ for the spatial unit Ω.
5. Resample (with replacement) the independent variables $x_i,\ i=24,25,27$ from their respective EDFs.
6. Resample (with replacement) the remaining secondary climatic variables $\mathbf{M}_{\Omega r}^{t^*}$ from their respective conditional distribution functions (6.6).
7. Scale up all climatic variables according to the scenario conditions. Check additional constraints. In case they are not fulfilled return to step 6.
8. Estimate $Q_{\Omega kr}^{t^*}=f\left(\mathbf{G}_{\Omega}^{t},\mathbf{U}_{\Omega r}^{t^*},\mathbf{M}_{\Omega r}^{t^*},\hat{\boldsymbol{\beta}}_k\right)\ \forall k=(2,3,4,5,6,9,10,11,12,14)$. With $\hat{\boldsymbol{\beta}}_k$ and $f(\bullet)$ according to Chapters 4 and 5.
9. Repeat step 2. T times.
10. Estimate the long-term mean for each realization $\overline{Q}_{kr}^{*}=E\left[Q_{\Omega kr}^{t^*}\right]\ \forall k,r\ \ t=1,\ldots,T$.
11. Repeat step 1. R times.
12. Estimate means and variances for each runoff characteristic at each time interval t, $\overline{Q}_{kt}^{*}=E\left[Q_{\Omega kr}^{t^*}\right]\ \ \forall t,k\ \ r=1,\ldots,R$, and

    $$\mathrm{var}(Q_{kt}^{*})=E\left[\left(Q_{\Omega kr}^{t^*}-\overline{Q}_{kt}^{*}\right)^2\right]\ \ \forall t,k\ \ r=1,\ldots,R\,.$$

13. Estimate $Q_k^{*}=E\left[Q_{kr}^{*t}\right]\ \forall k,\ t=1,\ldots,T\ \ r=1,\ldots,R$.
14. For each k, estimate from the simulated-EDF for the long term means $\left\{(Q_{kr}^{*}):r=1,\ldots,R\right\}$ the exceedance probabilities α_k with respect to historical records as

    $$\alpha_k=1-\frac{r}{R+1}\,,\quad Q_{k(r-1)}^{*}\leq E\left[Q_{\Omega k}\right]<Q_{k(r)}^{*}$$

15. For each k, estimate 95% confidence intervals based on $\left\{(Q_{kr}^{*}):r=1,\ldots,R\right\}$.

6.3 Model Implementation

6.3.1 Special Study Area

The proposed simulation model will be applied in the spatial unit No. 13, which is located upstream of the station Denkendorf-Sägewerk (E3 526 300, N5 397 100) in the river Körsch. Its area is about 126.3 km² and because of its vicinity to Stuttgart it has endured a rapid land use and cover change in the past four decades. Figure 6.2 shows the location of the Special Study Area as well as the main transportation network and main settlements in the region.

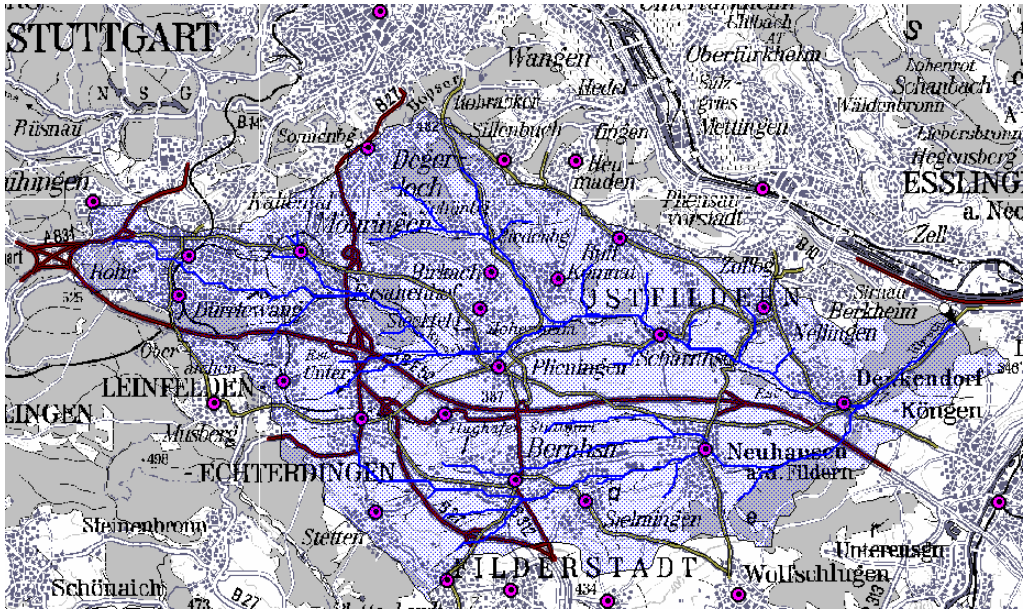

Figure 6.2 Special Study Area for the land use and cover change simulation model.

Stuttgart is the capital of the State of Baden-Württemberg as well as the state's Central Business District, and the main cultural and industrial hub of the Greater Stuttgart Region, which is composed of the following counties (*Landkreis*) Böblingen, Esslingen, Göppingen, Ludwigsburg, and Rems-Murr, as well as the independent municipality (*Stadtkreis*) Stuttgart. This region is considered a densely populated area (BBR, 2000), with a gross density in 2001 of about 717 inh/km² (SLA).

Stuttgart municipality provides an oversupply of jobs since its activity rate (i.e. $Total\,Employment : Total\,Population$) is about $3:5$, whereas the region has an average of about $1.8:5$ (in 2001, SLA). This large difference in the employment distribution, as well as the variety of services offered in the central city, constitute the main driving forces for daily commuting to Stuttgart.

6.3.2 Calibration and Validation of the LUCC Model

The LUCC model proposed before will use four (i.e. $u = 3$) mutually exclusive land use/cover classes, namely

Table 6.1 Land use/cover categories.

q	**Description**
0	restricted or unused land
1	forest
2	impervious cover
3	permeable area

The procedure to calibrate the model comprises the following steps. The first step is the definition of the potential predictors. According to (6.3), the probability $p_{ij}^{t}(q,q')$ has to be explained by exogenous variables called driving forces. In the present case, six potential predictors have been conceived as proximate sources of a land use/cover change. They denote accessibility to main transportation axes, jobs, amenities (located in towns and settlements) as well as morphological variables. In this model, it is assumed that such variables remain unchanged during the simulation period. A summary of these variables is shown Table 6.2. All variables have been defined as lattices $x_k(i,j) : (i,j) \in \mathbf{Z}$.

Having done this, the available land use/cover images acquired in 1975 and 1993 respectively (see Section 2.6.1) were used to determine all sites where land use/cover transitions ($q \rightarrow q'$, $\forall q,q' > 0$) have taken place during this period. As a result, it was found that the number of cells with transition $(2,1)$ is negligible (i.e. 0.08%). This implies that the probability of a transition from impervious cover to forest can be taken as approximately equal to zero. Moreover, it is assumed that it will remain constant during the simulation period for all cells in the Special Study Area.

Table 6.2 Potential predictors of land use/cover change.

k	**variable**	**Description**	**Units**	**Source**
1	$x_1(i,j)$	Distance to main highways	[m]	Digitized 1:50 000 topographic maps
2	$x_2(i,j)$	Distance to towns and settlements with metro or railway connection	[m]	Digitized 1:50 000 topographic maps
3	$x_3(i,j)$	Distance to streams	[m]	From DEM, 30×30m
4	$x_4(i,j)$	Elevation	[m]	DEM, 30×30m
5	$x_5(i,j)$	Slope	[°]	From DEM, 30×30m
6	$x_6(i,j)$	Aspect relative to south	[°]	From DEM, 30×30m

Then, five independent random samples, one for each possible land use/cover transition (q,q'), were obtained according to the following criteria. Each sample should include a binary indicator variable $y_{qq'}(i,j)$ and the corresponding values of the exogenous variables $x_k(i,j)$, i.e. each sample is composed of the following information $\left\{\left(y_{qq'}(i,j), x_1(i,j),\ldots,x_6(i,j)\right) : (i,j) \in \mathbf{Z}\right\}_{qq'}$. Additionally,

each sample should have an equal number of observations for each category of the binary indicator, and a total of $\mathrm{nobs} = 2000$. The binary indicator variable denotes the probability of occurrence of a land use/cover change. If it has occurred it takes the value 1, if not it takes the value 0. More formally

$$y_{qq'}(i,j) = \begin{cases} 1 & \text{if } U_{ij}^{t1} = q' \wedge U_{ij}^{t0} = q \wedge q \neq q' \\ 0 & \text{if } U_{ij}^{t1} = U_{ij}^{t0} = q \end{cases}, \tag{6.7}$$

where $t0 = 1975$, and $t1 = 1993$.

The calibration of the parameters needed for (6.3) will be carried out for each transition probability independently. The explained variable is the binary indicator whereas the explanatory variables are the driving forces x_k. A model for a transition probability (q, q') assumes that the observations of the binary indicator provided by the corresponding sample are realizations of a Bernoulli distribution. The expectation of this variable is therefore

$$E\left[y_{qq'}(i,j)\right] = \Pr(q,q') = \frac{e^{\eta(x_k)}}{1+e^{\eta(x_k)}}, \tag{6.8}$$

where $\eta(x_k)$ is the linear predictor (see Chapter 4) defined as

$$\eta(x_k) = \beta_0(q,q') + \sum_{k=1}^{K} \beta_k(q,q') x_k(i,j). \tag{6.9}$$

Upon this basis, the best models where obtained by applying the method described in Chapter 3 to select the best model given K predictors. The coefficients were fitted by the maximum likelihood method (Chapter 4). The results for the most robust models are shown in Table 6.3. All variables are significant at the 5% level.

Table 6.3 Fitted model coefficients for each transition probability.

Land use/cover transition		$\hat{\beta}_0(q,q')$	$\hat{\beta}_1(q,q')$	$\hat{\beta}_2(q,q')$	$\hat{\beta}_4(q,q')$	$\hat{\beta}_5(q,q')$
From (q)	**To** (q')					
1	2	5.966E -01	7.030E-03	-9.173E-02	-1.259E-03	-1.768E-03
1	3	5.561E+00	-9.179E-03	-8.639E-02	-5.745E-04	-7.529E-04
2	3	3.027E+00	-1.018E-02	-8.011E-02	-8.123E-05	9.876E-04
3	1	-3.168E+00	4.267E-03	1.798E-01	-2.508E-04	5.638E-04
3	2	-3.678E+00	1.227E-02	3.160E-02	-9.757E-04	-5.455E-04

In order to validate the model, a land use/cover map from 1984 (see Section 2.6.1) has been used as a starting condition. Then, using the parameters shown in Table 6.3 and corresponding scaling parameters, the model was run for an interval of 9 years with an $R = 100$. As a result, one hundred realizations for the land use/cover state in 1993 were obtained and compared with the observed land cover map from 1993 using the standard error matrix. On average, the realizations have shown that the model has an overall accuracy of 85%.

6.4 Development Scenarios for the Special Study Area

The proposed LUCC model as well as the hydrological models found before (see Chapters 4 and 5) will be coupled during the simulations under the framework conditions of a given scenario for the Special Study Area (see Figure 6.2).

Scenarios are "*neither predictions nor forecasts of future conditions. Rather they describe alternative plausible futures that conform to sets of circumstances or constraints within which they occur*" (Hammond, 1996). The purpose of scenarios "*is to illuminate uncertainty, as they help in determining the possible ramifications of an issue along one or more plausible (but indeterminate) paths"* (Fisher, 1996). Scenarios to be conceived for this study will have a dynamic character because they "*not only look into consistent future situations, but* [also] *include the consideration of feasible development paths*" (Treuner, 1995). This character of a given scenario will be accomplished in this study by using a stochastic simulation, which will deliver a number of "images of possible futures" given a common starting situation. According to Treuner (1995), scenarios must be envisaged and elaborated taking into account three fundamental issues: 1) future social values; 2) interpretation of a region's external conditions; and 3) assumptions (explicit or implicit) as to the mechanisms of causes and effects of changing patterns.

It should be noted that the third point has been already carefully analysed in the context of the present study. For instance, cause-effect relationships have been found between many runoff characteristics and the shares of the land cover, morphological, and climatic variables for a given basin. Besides that, the land cover state of a given basin at a point in time has been related with exogenous variables governing land use/cover change. The fundamental hypothesis in this case is that these models fitted with past information will still be valid in the future. The remaining two issues are to be discussed below.

6.4.1 Socio-economic Scenarios

In order to simplify the analysis and taking into account the actual socio-economic and political situation in Germany, only two future paths with regard to socio-economic factors and attitudes have been conceived for the Special Study Area. They have been termed as Scenarios S1 and S2. These scenarios have some common features to ease comparison. For instance, the population in the region will slightly decline at about 0.1% per year (according to an external forecast for the administrative units covering the Special Study Area i.e. Stadtkreis Stuttgart and Landkreis Esslingen, SLA, 2002). Furthermore, the GDP per capita of Baden-Württemberg will grow at an average rate of about 2.3% per year (SLA). However, these scenarios will have characteristic conditions with regard to the driving forces and the society attitudes that promote land use/cover changes, namely:

Scenario S1

The keyword for this scenario is status quo. The storyline of this scenario describes a future state of the Special Study Area in which its development can be explained as an extrapolation of past trends. This scenario assumes that the steady growth of income per capita combined with an excellent provision of road transportation network and stable taxation for fossil fuels (0.65 €/l) will keep the relationship between car-ownership and the demand for residential floor space tightly correlated

(r^2=0.88 from 1974 to 1997, as can be seen in Figure 2.2). These indicators will continue to grow at 2.6% and 1.5% per year respectively. In addition to that, the rent for housing in Stuttgart and its surroundings will soar due to the region's high level of centrality.

The implication of these assumptions is that although the population settled in the region is quasi constant, the demand for larger apartments and detached houses with large gardens located in villages and settlements with good road accessibility will grow rapidly. As a result, new housing areas will appear everywhere in the outskirts of Stuttgart, accompanied by large shopping malls with huge parking places whilst floor space downtown will be swiftly taken by branches of the service sector.

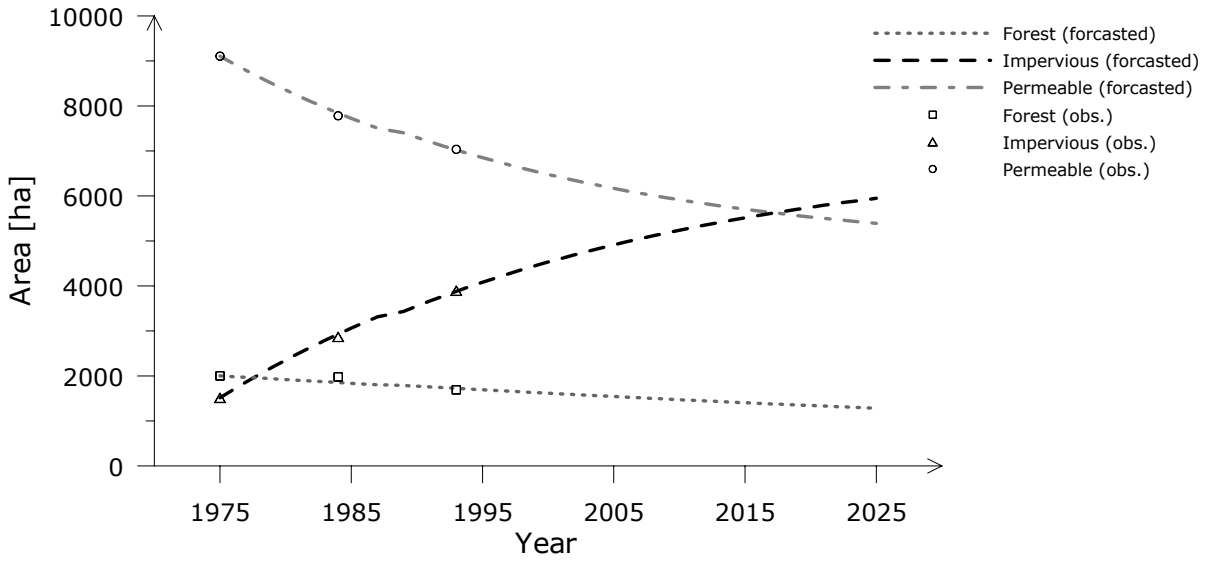

Figure 6.3 Land use/cover forecast based on Scenario S1 conditions for Special Study Area as a whole (total area 126.3 km²). The observation points are derived from the LANDSAT scenes for 1975, 1984 and 1993. The forecasted period is up to 2025.

The consequences of these developments for the overall balance of the land use/cover in the Special Study Area can be seen in Figure 6.3. The forecast has been done based on a Markov chain whose transition matrix adjusted to fit the observations is

$$\mathbf{U}^{t+1} = \mathbf{U}^{t^{\mathrm{T}}} \begin{bmatrix} 1 & 0 & 0 & 0 \\ 0 & 0.984 & 0.016 & 0 \\ 0 & 0 & 0.986 & 0.014 \\ 0 & 0.002 & 0.018 & 0.980 \end{bmatrix}, \tag{6.10}$$

where $\mathbf{U}^t$ is a 4-dimention vector denoting the area for each land use/cover category for the whole Special Study Area in time t. Applying this procedure, only the last three land use/cover categories ($q = 1,\ldots,3$) will endure transformations, for instance, forest will decrease slightly, impervious areas will grow rapidly, and permeable areas will decrease continuously. Restricted areas are preserved. This scenario describes a fast urban sprawl in the Special Study Area. Using this forecast the LUCC model will be scaled up so that the land use/cover categories forest, impervious, and permeable cover will reach in average 1280, 5950, 5390 ha respectively by the end of 2025.

Scenario S2

The keyword for this Scenario is local sustainability. The storyline of this scenario differs from the previous one in several topics. Firstly, the public opinion, in general, and the political decision-making bodies, in particular, will finally become aware that a rapid urban sprawl represents a threat to the environment, which, in turn, may contribute to increased flooding and drought hazards in the region. Consequently, tougher land use by-laws and higher property tax regulations will be adopted. As a result, the demand for floor space per capita will be reduced significantly.

Secondly, the "Eco Tax" (tax on fuel that makes commuting more expensive) will be strengthened. Tax exceptions will be introduced for smaller and pollution-free cars, whereas higher taxes will be imposed on vehicles with standard combustion engines. These regulations, along with a sufficient frequency and capacity offered by almost pollution-free mass transportation systems, will slow down the growth rate of the car-ownership ratio. As a result, the demand for space required for new roads and parking places will be reduced dramatically. Because of the new legislation, the growth rate of impervious areas, as can be seen in Figure 6.4, will slowdown from 1.3% per year of the "status quo" Scenario to 0.4% per year in Scenario S2. The scenario denotes a consolidation of the urban fabric of the Special Study Area.

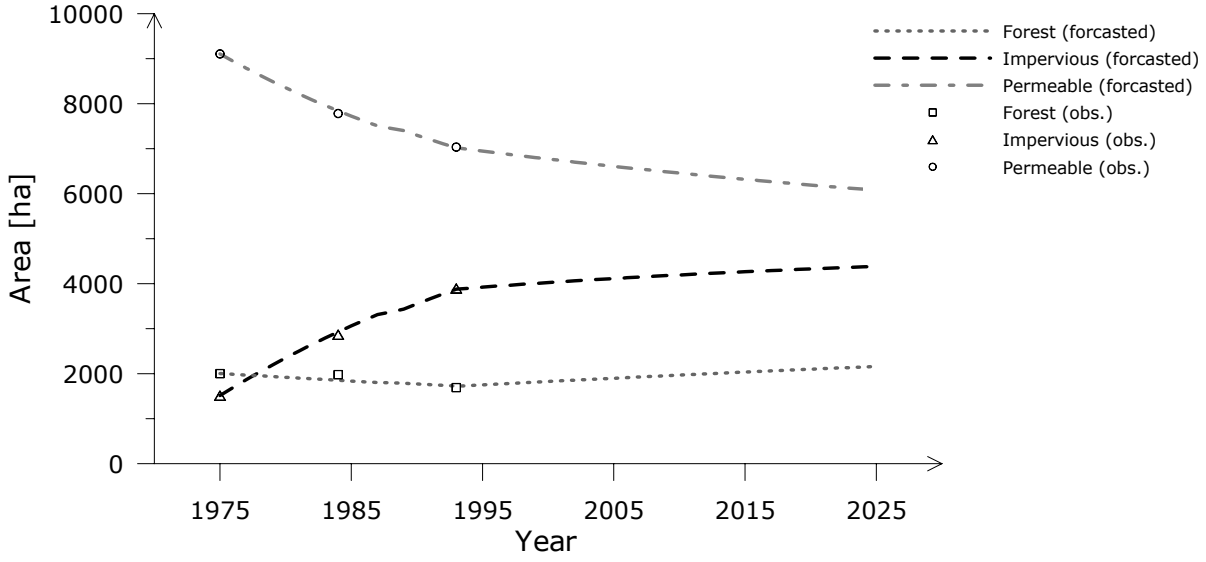

Figure 6.4 Land use/cover forecast based on Scenario S2 conditions for the Special Study Area as a whole.

Thirdly, the decrease of forest observed in the period 1975 to 1993 has been taken by the public opinion as a loss of German "identity". Therefore, land use/cover compensation rules stated in the EIA (Environmental Impact Assessment) by-laws will be strengthened, and wherever possible reforestation projects will be initiated. At the end of the simulation period (i.e. 2025) the land use/cover categories forest, impervious, and permeable cover will have an average of 2160, 4390, and 6075 ha respectively.

6.4.2 Macroclimatic Scenarios

Why are macroclimatic scenarios needed during these simulations? Before this question is answered, another question must be asked: Is climate really changing? The answer is unequivocally yes (Karl and Trenberth 1999, Houghton et al. 2001, Zwiers 2002). Currently, there is plenty of empirical evidence that the Earth's surface mean temperature has endured a very rapid increase during the last 100 years that "counters a millennial-scale cooling trend, which is consistent with long-term astronomical forcing" (Mann et al. 1999) (i.e. the gravitational driving force "which is thought to have driven long-term temperatures downward since the mid-Holocene at a rate within the range of -0.01° to -0.04°C/century" [see Berger,1988 in Mann et al. 1999]). As an example, Figure 6.5 depicts the reconstruction of the temperature anomalies[2] for the past millennium in the Northern Hemisphere carried out by Mann et al. (1999). Based on proxy data (i.e. paleoclimatic) and instrumental records from many studies (Hansen and Lebedeff 1988, Jones, 1994, Vinnikov et al. 1990, Mann et al. 1999) the IPCC (Houghton et al. 2001) has concluded that the average surface temperature in the Northern Hemisphere has increased by 0.6 ± 0.2°C during the 20th century.

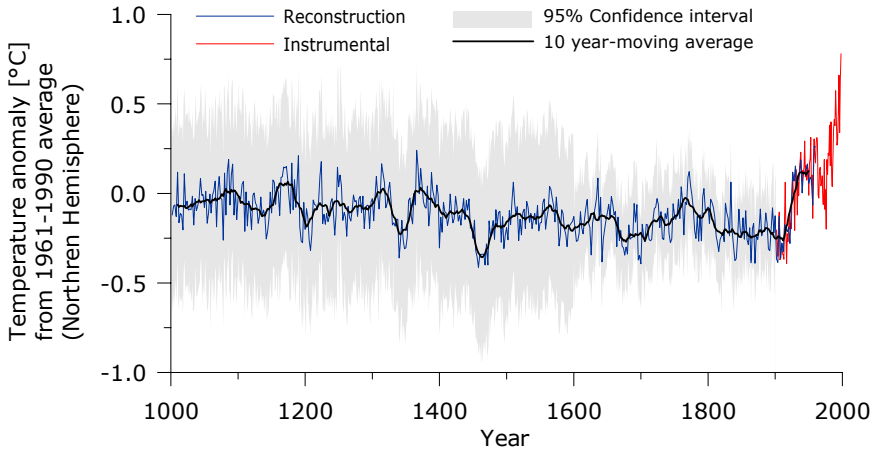

Figure 6.5 Reconstruction of the Northern Hemisphere average temperature anomaly for the past millennium according to Mann et al. 1999(2). Data from the period (1000 to 1902) is reconstructed from tree rings, ice cores, varved sediments, and corals [Mann et al. (1) 1999]. Data from period (1902-1998) is from instrumental measurements. The grey region represents the 95% confidence range. The moving average shows the decreasing trend up to 1900.

Since climate is changing, the weather and its meteorological indicators used in this study at mesoscale will certainly change in the future. However, to estimate how big these changes would be in a given place using General Circulation Models (GCM) is rather complicated because of the extremely high uncertainty involved in future estimates. The uncertainty of the system does not come only from the complexity of the system[3] itself but also from future actions of human beings, especially with

---

[2] The air temperature anomaly is defined as the difference between the temperature in a given year and the average from period (1961-1990), which is roughly 15°C for the Northern Hemisphere (IPCC, 2000).

[3] The intrinsic uncertainty of the state-of-the-art GCM models is caused by the complexity of the iterations among the components of the climatic system, i.e. the atmosphere, the hydrosphere, and the biosphere. At the moment, even using the best supercomputers available, the system of equations can be solved for a spatial resolution of about H: 250 km, V: 1 km. Hence, results of GCM cannot be used directly for climatic inferences at local level (Karl and Trenberth 1999). Estimates at local level are then obtained by statistical downscaling techniques (von Storch et al. 1999).

regard to both the amount of emissions of greenhouse gases into the atmosphere and the magnitude of land use/cover changes. Greenhouse gases (e.g. CH_4, N_2O, CO_2, SO_2) are directly linked with climatic disruptions of the last century. Figure 6.6 shows for example the strong correlation between the temperature anomalies of the Northern Hemisphere and the atmospheric concentration of CO_2 (r = 0.72).

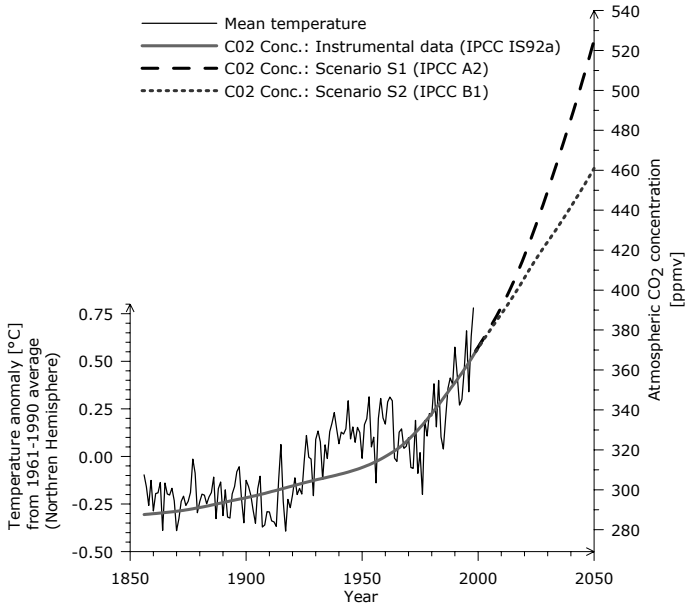

Figure 6.6 Relationship between the atmospheric CO_2 concentrations and the temperature anomalies in the Northern Hemisphere up to 1998. Additionally, this Figure depicts the emission conditions adopted in this study for scenario S1 and S2, which correspond to the IPCC emissions scenarios A2 and B1 respectively. [Data: temperature anomalies from Mann et al. 1999; CO_2 concentrations from the standard IPCC CO_2 concentration history dataset (Enting et al. 1994); IPCC scenario concentrations obtained from IPCC Data Centre].

Based on these facts, the answer to the first question is now straightforward. Macroclimatic scenarios are needed in order to deal with the uncertainty of climate in the future. They will provide the framework for the climatic conditions for a future world under given hypothesised socio-economic and emission scenarios. In order to simplify the analysis, this study only conceives two extreme macroclimatic scenarios called Scenario C1 and C2 respectively.

Scenario C1

The keyword for this scenario is pessimistic, and describes the worst-case situation. The storyline for this emission scenario corresponds to the "A2" scenario described by Jordan et al. (2000) and McCarthy (2001). It envisages a heterogeneous future world with a continuously growing population. Emphasis is given to local, short-term solutions instead of long-term, globally-oriented, and sustainable ones. Free market, consumerism, and increase of income per capita are pursued all over the world. The promotion of clean and resource-efficient technologies will be very limited, and the main source of energy will still be fossil fuels. Global inequality will grow. Under these conditions, it is hypothesized that the atmospheric CO_2 concentration will reach about 525 ppmv by the year 2050.

Put differently, this scenario assumes that Nature is very resilient to human stress; that global warming is a natural process in which anthropogenic activities do not play a significant role; and that sustainability is a rather expensive and unachievable goal.

GCM simulations (CGCM1: Boer et al., 2000; and HadCM2: Johns, 1996) under this emission scenario suggest that 30-year mean climate changes at regional levels will be very likely to happen in the future. For Germany in particular, the most expected climatic disruptions in the future are summarized below (for details see also Table 6.4).

Precipitation will increase in winter due to an intensified hydrological cycle but will decrease in summer because of an increased evapotranspiration. Furthermore, the intensity and frequency of extreme precipitation events in summer will likely increase, mainly because of changes in atmospheric moisture, thunderstorm activity, and large-scale storm activity. (Hennessy et al., 1997; McGuffie et al., 1999). In other words, the return period of extreme events will be shortened. Consequently, magnitude and frequency of high flows will most likely increase. It is also very likely that low-flow periods or droughts will increase due to greater evaporation (Gregory et al., 1997). Mean temperature will very likely increase in both seasons. The frequency of minimum and maximum temperatures will also change, i.e. fewer cold and frost days in winter, and much dryer and hotter days in summer (Houghton et al. 2001). In other words, weather patterns in this future world will become more intense and erratic.

Scenario C2

The keyword for this scenario is optimistic. The storyline of this emission scenario corresponds to scenario "B1" described by Jordan et al. (2000) and McCarthy (2001). It describes a convergent future world with a global population stabilizing in mid-century. "Global Sustainability" is the motto of all governments on Earth, which implement global solutions for economic and environmental issues. Most of the energy demand will be covered by renewable energy sources (e.g. biomass, solar, hydroelectric, tidal power, eolic, and geothermic). Promotion of clean and resource efficient technologies will be a key element of the decision-making process. As a result, CO_2 emissions as well as other greenhouse gasses will decrease after 2050, and the atmospheric CO_2 concentration will reach about 550 ppmv only by the year 2100.

The GCM (CGCM1: Boer et al., 2000; and HadCM2, Johns 1996) fed with these conditions predict that the climatic changes in Germany will be much less severe than those in scenario C1; in fact, the difference between these scenarios in growth rate per decade for both mean precipitation and temperature is in relation of 3:1 approximately. The mean temperature increase, for instance, by the year 2020 will remain under the 95% confidence interval of the natural variability (McCarthy, 2001), but the change of mean precipitation in winter will certainly exceed the natural variability of the last century (about 0.1% per decade, New et al., 2000). The detailed information obtained from these simulations is shown in Table 6.4.

6.4.3 Assembling the Development Scenarios

The assessment of the future state of a complex system requires a starting point situation and a reference framework from which the system will evolve into the future, i.e. a development scenario. In the present case, the starting point is the state of the catchment of the river Körsch in 1993. The

development scenarios will be assembled by combining one socio-economic scenario (S1, S2) with one macroclimatic scenario (C1, C2) at a time. As a result, four development scenarios are obtained, which are called C1S1, C1S2, C2S1, and C2S2 respectively. The specific conditions for each of them are shown Table 6.4.

Table 6.4 Composition of the development scenarios.

Variable			**Development Scenario**			
Description	**Name**	**Class / Season /Cat.**	**C1S1**	**C2S1**	**C1S2**	**C2S2**
Land-cover			Change [% / year]			
	x_{17}	Forest	-0.9	-0.9	+0.7	+0.7
	x_{18}	Impervious cover	+1.3	+1.3	+0.4	+0.4
	x_{19}	Permeable cover	-0.8	-0.8	-0.5	-0.5
Mean precipitation[II] $\{x : F(x) < 0.9\}$			Change [% / decade]			
	x_{24}	Winter	+4.1	+1.6	+4.1	+1.6
	x_{25}	Summer	-2.7	-1.0	-2.7	-1.0
Low precipitation[II] $\{x : F(x) \leq 0.1\}$			Probability of occurrence[I] $\Pr(X \leq x)$ [-]			
	x_{24}	Winter	*	*	*	*
	x_{25}	Summer	0	*	0	*
High precipitation[II] $\{x : F(x) \geq 0.9\}$			Change in probability and magnitude [% / decade]			
	x_{24}	Winter	*	*	*	*
	x_{25}	Summer	+4.0	*	+4.0	*
Mean temperature[II] $\{x : F(x) < 0.9\}$			Change [% / decade]			
	x_{30}	Winter	+2.1	+0.8	+2.1	+0.8
	x_{31}	Summer	+2.9	+1.1	+2.9	+1.1
Low temperature[II] $\{x : F(x) \leq 0.1\}$			Probability of occurrence[I] $\Pr(X \leq x)$ [-]			
	x_{30}	Winter	0	*	0	*
	x_{31}	Summer	0	*	0	*
High temperature[II] $\{x : F(x) \geq 0.9\}$			Change in probability and magnitude [% / decade]			
	x_{30}	Winter	*	*	*	*
	x_{31}	Summer	+10.0	*	+10.0	*
Annual precipitation[III]			Change [% / decade]			
	x_{21}	Winter	+3.9	+1.6	+3.9	+1.6
	x_{22}	Summer	-2.7	-1.0	-2.7	-1.0
Maximum API[III]			Change [% / decade]			
	x_{27}	Annual	+1.4	+0.5	+1.4	+0.5
	x_{28}	Winter	+3.9	+1.5	+3.9	+1.5
	x_{29}	Summer	0.0	0.0	0.0	0.0
Maximum Temperature[III]			Change [% / decade]			
	x_{32}	Winter	+2.0	+0.7	+2.0	+0.7
	x_{33}	Summer	+1.6	+0.6	+1.6	+0.6
ATI at annual peak[III] discharge			Change [% / decade]			
	x_{34}	Annual	-0.2	-0.1	-0.2	-0.1
Duration of a given category of Circulation Patterns[III, IV]			Change [% / decade]			
	x_{41}	Winter / Wet	+6.9	+2.7	+6.9	+2.7
	x_{40}	Summer / Wet	-8.9	-3.5	-8.9	-3.5
	x_{38}	Summer / Dry	+9.0	+3.3	+9.0	+3.3

Notes: * Denotes that there will be no significant change in magnitude or that the probability of occurrence will remain equal to that of the reference period 1961-1993.

I Based on the PDF of the variable during the reference period.

II Based on GCM simulations carried out by IPCC (CGCM1: Boer et al., 2000; and HadCM2: Johns, 1996) under a given emission scenario.

III Based on potential relationships between a given variable and mean precipitation and mean temperature at catchment level. Winter, summer, and annual relationships are

$$x_i^t = \beta_0 \left(x_{24}^t\right)^{\beta_1} \left(x_{30}^t\right)^{\beta_2} + \varepsilon_i^t$$

$$x_i^t = \beta_0 \left(x_{25}^t\right)^{\beta_3} \left(x_{31}^t\right)^{\beta_4} + \varepsilon_i^t$$

$$x_i^t = \beta_0 \left(x_{24}^t\right)^{\beta_1} \left(x_{30}^t\right)^{\beta_2} \left(x_{25}^t\right)^{\beta_3} \left(x_{31}^t\right)^{\beta_4} + \varepsilon_i^t$$

respectively. This formulation has the advantage that can be easily transformed into an incremental equation. For example, for winter the incremental equation is

$$\Delta x_i^t = \beta_1 \Delta x_{24}^t + \beta_2 \Delta x_{30}^t .$$

The parameters β_i were found empirically and all are significant at the 5% level. The following Table shows these coefficients for each variable:

Variable	β_1	β_2	β_3	β_4
x_{21}	0.956	0.026		
x_{22}			0.862	-0.131
x_{27}	0.290	0.017	0.475	0.508
x_{28}	0.945	0.048		
x_{29}			0.808	0.765
x_{32}	0.125	0.703		
x_{33}			-0.042	0.516
x_{34}	-0.032	0.004	0.020	0.009
x_{38}			-2.492	0.677
x_{40}			2.796	-0.603
x_{41}	1.483	0.361		

IV This fact is also supported by the excellent agreement found between observed and downscaled monthly precipitation at catchment level (Bardossy and Caspary, 1999) using the CPs.

6.5 Simulation Results

A total number of 2500 realizations have been carried out for each development scenario (simulation time $\sim$ 7.5h on an 800 MHz workstation). Based on the simulation results, the following summary has been prepared to show how the conditions of each scenario have influenced the runoff characteristics of the Special Study Area, however, a more detailed analysis of results and conclusions will be presented in Chapter 8.

Firstly, Table 6.5 shows the average growth rate in percent per decade for each simulated variable and for each scenario, taking as reference year the beginning of the simulation, i.e. 1994. This information is presented in both a tabular and a visual way to ease the comparison between different scenarios and types of impact measured by the simulated variables. Based on this optical aid, it can be clearly seen that the hydrological system of the studied catchment will endure the greatest disruptions under the C1S1 scenario conditions, and conversely, the least ones under scenario C2S2. The other two scenarios, i.e. C1S2 and C2S1, are in-between the previous two.

Table 6.5 Average percent change per decade for each simulated variable taken 1994 as reference year. The colours indicate the magnitude and the sign of the simulated changes (see legend below); e.g., red represents the highest positive change whereas dark blue does the opposite.

Variable Description	Symbol	Development Scenario				Development Scenario			
		C1S1	C1S2	C2S1	C2S2	C1S1	C1S2	C2S1	C2S2
Total discharge in winter	Q_2	6.9	5.4	3.7	2.4				
Total discharge in summer	Q_3	-2.6	-6.8	0.4	-4.1				
Specific peak in winter	Q_4	8.8	5.4	5.4	2.5				
Specific peak in summer	Q_5	-3.7	-1.6	0.1	-0.6				
Specific volume of the annual peak	Q_6	9.9	3.2	8.0	2.2				
Total duration of high flows in winter	Q_9	5.6	6.2	2.3	2.7				
Total duration of high flows in summer	Q_{10}	-1.9	-4.5	1.8	-1.1				
Frequency of high flows in winter	Q_{11}	7.1	3.5	4.4	1.3				
Frequency of high flows in summer	Q_{12}	-2.8	-2.6	-1.2	-1.8				
Total drought duration in summer	Q_{14}	8.4	8.0	3.7	3.8				

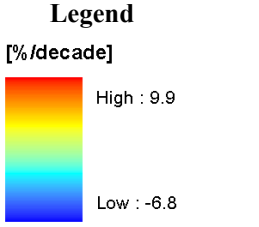

Each average growth rate has been estimated based on the simulated mean values for 1994 and 2025. This approach yields satisfactory approximation of the decadal growth rates since the simulated mean value grows continuously during the simulation period as can be seen in Figure 6.7.

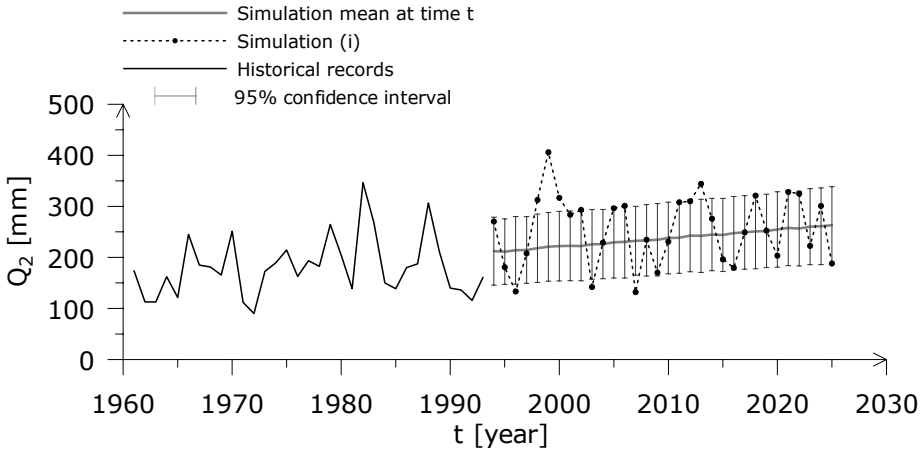

Figure 6.7 Historical records for total winter discharge (Q_2) in the Special Study Area from 1961 to 1993. The dotted line on the right depicts one of the realizations of this variable for the period 1994 to 2025 under C1S1 scenario conditions. The continuous line denotes the simulated mean value at a give time t, which has a positive trend in this case (i.e. 6.9% per decade, see Table 6.5).

From the simulations, it is also possible to estimate the likelihood that the long-term mean of a given variable will be exceeded during the period 1994-2025 under a given scenario. The summary of these exceedance probabilities and the long-term means (i.e. from 1961 to 1993) for each variable and scenario are presented in Table 6.6. If the probability is greater than 0.95, this means that it is very likely that the past mean of a given variable will be surpassed in the future, or in other words, that the expectation of a variable will increase over time. On the contrary, a value less than 0.05 will mean that the past mean of a variable will be hardly reached (in fact it will only occur 5% of the time at this probability level), thus, a decreasing tendency of the expectation of such a variable is very likely foreseeable.

Table 6.6 Probability that the long-term mean for a given variable will be exceeded under certain scenario conditions.

Variable Description	Symbol	Long-term mean	Unit	Development Scenario			
				C1S1	C1S2	C2S1	C2S2
Total discharge in winter	Q_2	181.2	[mm]	1.000	1.000	1.000	1.000
Total discharge in summer	Q_3	153.4	[mm]	0.332	0.020	0.238	0.020
Specific peak in winter	Q_4	7.1	[mm]	0.218	0.037	0.052	0.002
Specific peak in summer	Q_5	9.1	[mm]	0.335	0.335	0.231	0.229
Specific volume of the annual peak	Q_6	25.8	[mm]	1.000	0.992	1.000	0.973
Total duration of high flows in winter	Q_9	10.0	[day]	0.732	0.775	0.580	0.649
Total duration of high flows in summer	Q_{10}	8.1	[day]	1.000	0.995	0.998	0.984
Frequency of high flows in winter	Q_{11}	4.3	[-]	0.920	0.712	0.786	0.460
Frequency of high flows in summer	Q_{12}	4.9	[-]	0.265	0.219	0.071	0.060
Total drought duration in summer	Q_{14}	21.2	[day]	0.437	0.423	0.703	0.716

The long-term means for both simulated and observed values for each runoff characteristic can also be plotted in order to visualize the effects of a given development scenario on a given runoff characteristic. In the present case the deviation from the mean of the historical records (1961-1993) expressed in percent has been found appropriate for this purpose. In addition to the magnitude of the deviation, which is shown in Figure 6.8 by a dot, it is also very important to know the degree of

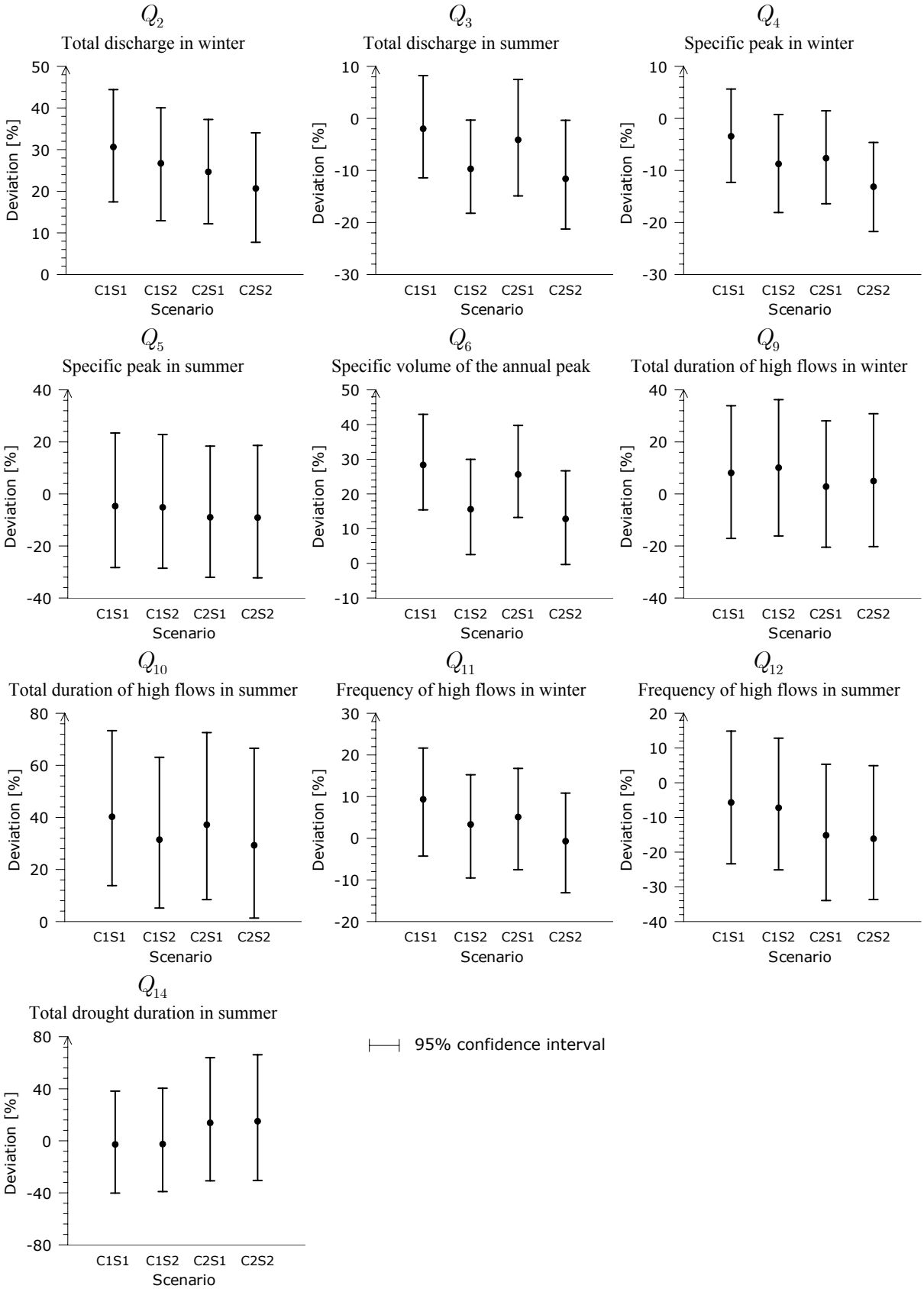

Figure 6.8 Deviations in percent of the mean of the simulated variables with respect to the respective historical mean (i.e. observations during 1961-1993) under given scenario conditions. The mean value and its 95% confidence interval are represented here with a dot and a bar respectively.

dispersion of this indicator. This has been achieved by plotting the 95% confidence interval of the simulated mean with respect to the reference period.

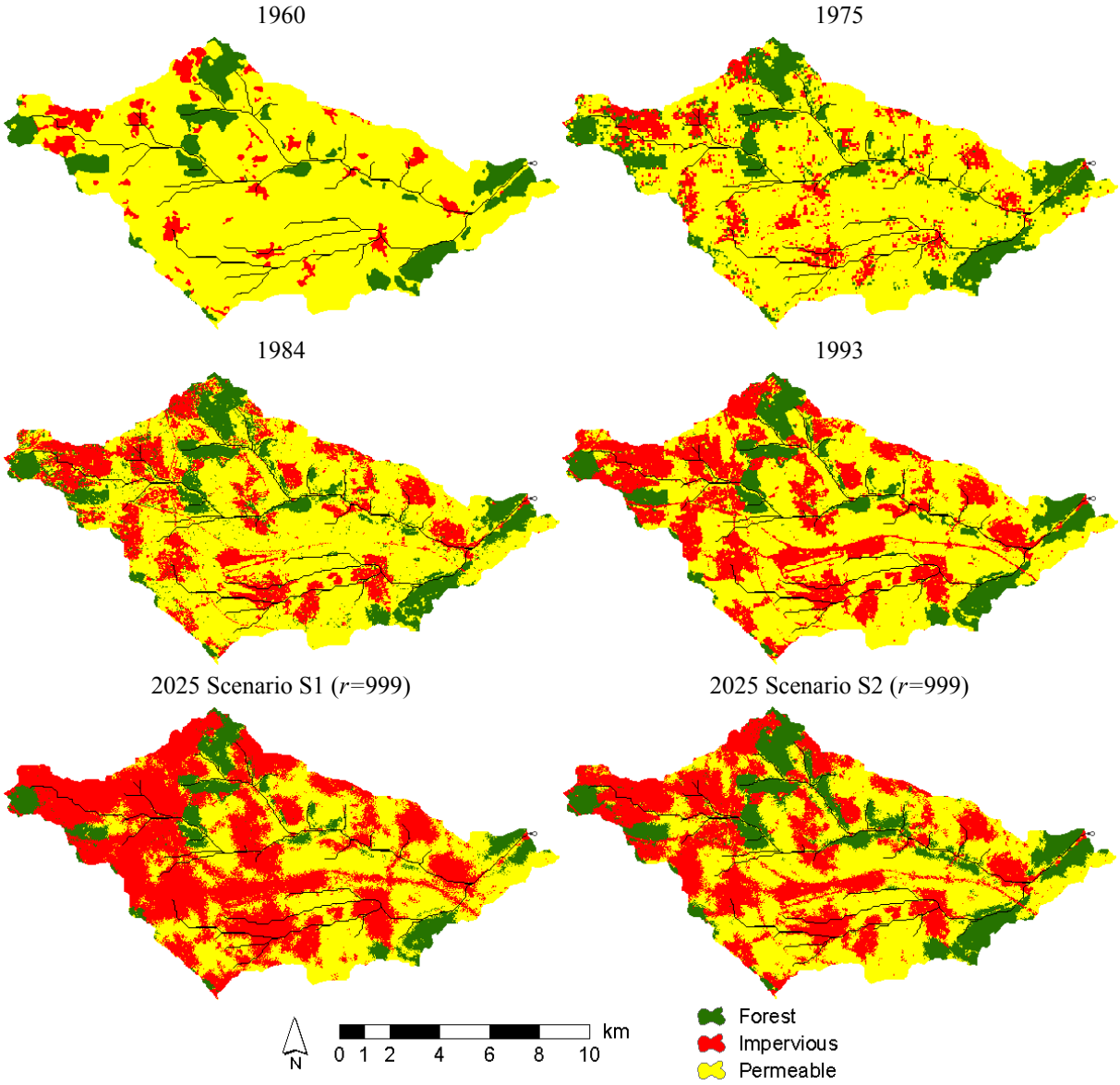

Figure 6.9 Time series of land cover in the Special Study Area from 1960 to 1993. Additionally, random realizations of the land use/cover for the year 2025 under two different scenario conditions.

As said above, 2500 land use/cover realizations were conducted for each scenario. The spatial domain of the catchment was divided into cells of 30×30 m with a total extension of 745 cells in west-east direction and 393 cells in north-south direction. The state of each land use/cover category for each cell has been reckoned during the simulation period based on the model proposed before. The land use/cover balance in the basin is estimated after each LUCC simulation has been finished. A sample of such results can be seen in Figure 6.10. These simulated values are subsequently employed for the evaluation of the runoff characteristics at the correspondent point in time. The results of the LUCC simulation, however, were not kept in order to speed up the simulation. The model, nevertheless, can deliver one of such realizations at a certain point in time, as can be seen in Figure 6.9 for socio-economic scenarios S1 and S2 respectively.

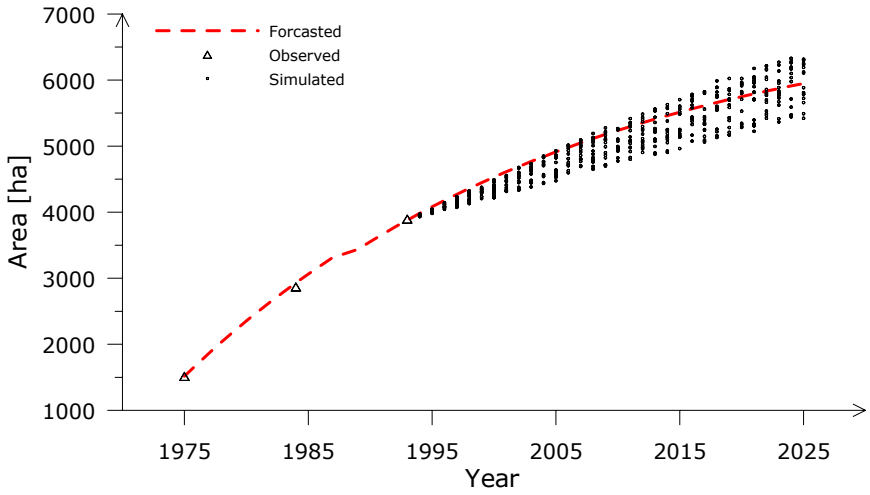

Figure 6.10 Sample from the land use/cover simulations showing the evolution of impervious cover in the Special Study Area based on socio-economic scenario S1. The forecasted trend and the observations have been depicted as a reference.

Additionally, the probability that the land use/cover state of a given cell will be transformed to a different state during the time span of the simulation can be estimated from the simulation results. Figure 6.11 shows, for instance, the spatial distribution of the probability that the land use/cover in a given location of the basin will be transformed to impervious cover by the end of 2025. In this Figure, for instance, the red colour indicates that the probability that a cell would be transformed to impervious cover (e.g. road, urban settlement) is greater than 0.9. This situation, as shown in this Figure, tends to occur mainly in the fringes of existing settlements were available land with particular morphological and accessibility conditions remains still under other usages.

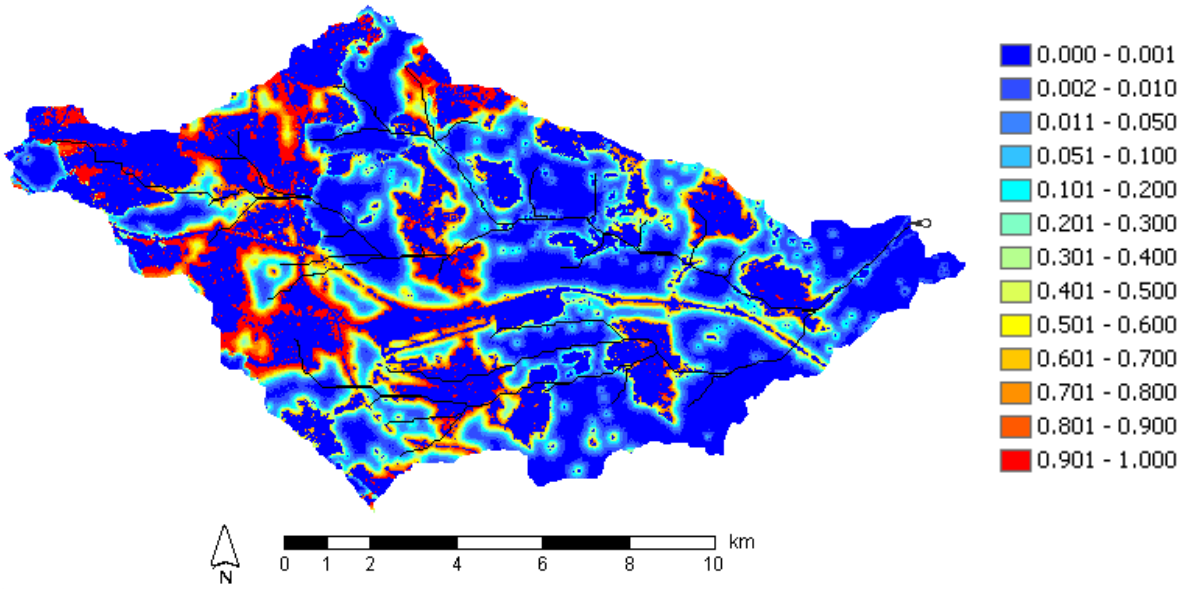

Figure 6.11 Probability that the land use/cover of a given location will be transformed to impervious cover up to the year 2025 based on the socio-economic scenario S1. (The sample size for each cell is 2500).